

See discussions, stats, and author profiles for this publication at: <https://www.researchgate.net/publication/236689076>

Glucose–Oxidase Label–Based Redox Cycling for an Incubation Period–Free Electrochemical Immunosensor

ARTICLE *in* ANALYTICAL CHEMISTRY · MAY 2013

Impact Factor: 5.64 · DOI: 10.1021/ac400573j · Source: PubMed

CITATIONS

23

READS

23

3 AUTHORS, INCLUDING:



Amardeep Singh

IndianOil

14 PUBLICATIONS 145 CITATIONS

SEE PROFILE



Haesik Yang

Pusan National University

114 PUBLICATIONS 2,445 CITATIONS

SEE PROFILE

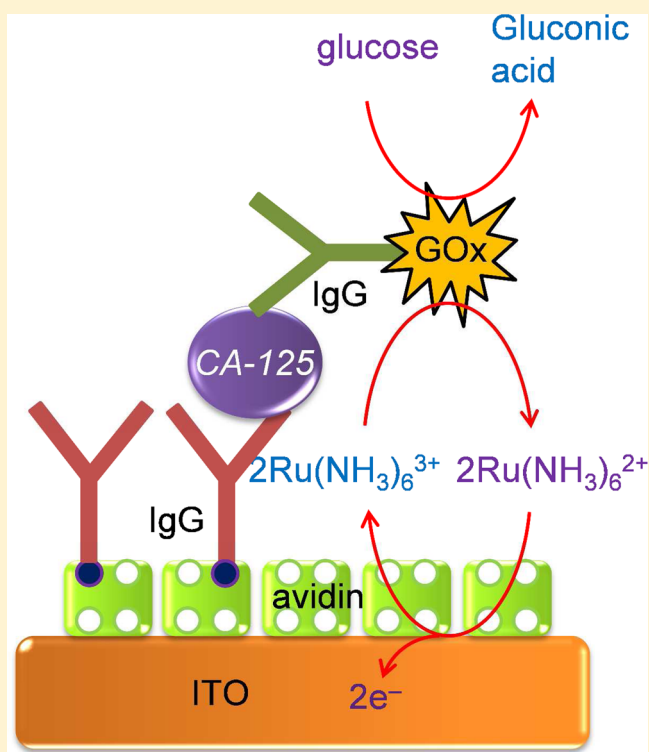
Glucose-Oxidase Label-Based Redox Cycling for an Incubation Period-Free Electrochemical Immunosensor

Amardeep Singh, Seonhwa Park, and Haesik Yang*

Department of Chemistry and Chemistry Institute of Functional Materials, Pusan National University, Busan 609-735, Republic of Korea

Supporting Information

ABSTRACT: Catalytic reactions of enzyme labels in enzyme-linked immunosorbent assays require a long incubation period to obtain high signal amplification. We present herein a simple immunosensing scheme in which the incubation period is minimized without a large increase in the detection limit. This scheme is based on electrochemical-enzymatic (EN) redox cycling using glucose oxidase (GOx) as an enzyme label, $\text{Ru}(\text{NH}_3)_6^{3+}$ as a redox mediator, and glucose as an enzyme substrate. Fast electron mediation of $\text{Ru}(\text{NH}_3)_6^{3+}$ between the electrode and the GOx label attached to the electrode allows high signal amplification. The acquisition of chronocoulometric charges at a potential in the mass transfer-controlled region excludes the influence of the kinetics of $\text{Ru}(\text{NH}_3)_6^{2+}$ electrooxidation and also facilitates high signal-to-background ratios. The reaction between reduced GOx and $\text{Ru}(\text{NH}_3)_6^{3+}$ is rapid even in air-saturated Tris buffer, where the faster competitive reaction between reduced GOx and dissolved oxygen also occurs. The direct electrooxidation of glucose at the electrode and the direct electron transfer between glucose and $\text{Ru}(\text{NH}_3)_6^{3+}$ that undesirably increase background levels occur relatively slowly. The detection limit for the EN redox cycling-based detection of cancer antigen 125 (CA-125) in human serum is slightly higher than 0.1 U/mL for the incubation period of 0 min, and the detection limits for the incubation periods of 5 and 10 min are slightly lower than 0.1 U/mL, indicating that the detection limits are almost similar irrespective of the incubation period and that the immunosensor is highly sensitive.



Catalytic reactions of enzyme labels are used in enzyme-linked immunosorbent assays (ELISAs) to generate a large number of signaling species per target.^{1–3} The incubation period for catalytic reactions must be sufficiently long to obtain high signal amplification, i.e., low detection limit. An incubation period of more than 30 min is generally required for microplate-based ELISAs, whereas incubation periods exceeding 10 min are required in electrochemical immunosensors. In order to achieve fast, sensitive detection, it is essential to reduce the incubation period.

In the case where direct electron transfer between the electrode and enzyme label occurs, electrochemical reaction along with enzymatic reaction can be simultaneously achieved without the need for an incubation period. However, the achievement of such electron transfer in immunosensors is a formidable challenge owing to the large electron-hopping distance between the electrode and the redox center of the

enzyme label.^{4,5} Mediated electron transfer may be achieved when a redox mediator that conveys electrons between the electrode and the redox center is present in solution;^{4–8} i.e., enzyme label-based electrochemical-enzymatic (EN) redox cycling (denoted EN_L redox cycling in our previous report)³ occurs (Figure 1a). Horseradish peroxidase (HRP) is commonly used as an enzyme label for this purpose.^{6,8} However, an incubation period of more than 10 min has been used even in this case.

Ru complexes such as $\text{Ru}(\text{NH}_3)_6^{3+}$ undergo fast outer-sphere electron-transfer reactions at electrodes^{9,10} and fast electron-transfer reactions with redox enzymes.^{11–13} Glucose oxidase

Received: February 22, 2013

Accepted: April 27, 2013

Published: May 10, 2013



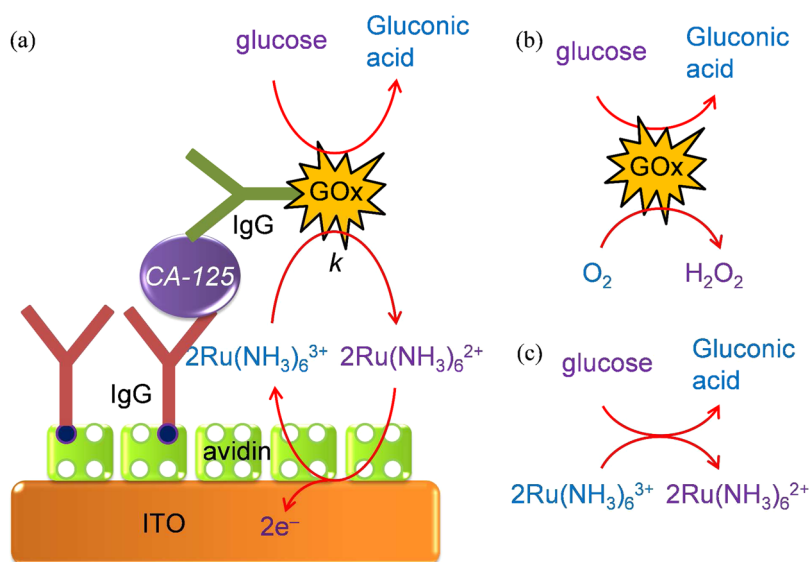


Figure 1. (a) Schematic of electrochemical immunosensor using GOx label-based EN redox cycling. (b) Enzymatic glucose oxidation by O_2 . (c) Direct electron-transfer reaction between glucose and $\text{Ru}(\text{NH}_3)_6^{3+}$.

(GOx) is one of the cheapest and most stable redox enzymes. Therefore, Ru complexes and GOx are commonly employed in mediated electron transfer as redox mediators and redox enzyme, respectively.^{4,11–14} For instance, Ru complexes and GOx have been successfully used for glucose detection using EN redox cycling.^{11,12} Although GOx has rarely been utilized as a label in immunosensors,^{15–17} it has often been used in conjunction with HRP for bienzyme-based signal amplification.^{18,19} However, the application of GOx label-based EN redox cycling to immunosensors has not been reported so far.

Herein, we report EN redox cycling using GOx as an enzyme label, $\text{Ru}(\text{NH}_3)_6^{3+}$ as a redox mediator, and glucose as a substrate and the application of the redox cycling to an incubation period-free immunosensor (Figure 1). The kinetics of the EN redox-cycling reaction and the unwanted side reactions in air-saturated solution are explored in relation to the signal-to-background ratio, and the optimal conditions for high signal-to-background ratio are investigated. The EN redox cycling is also applied to the detection of cancer antigen 125 (CA-125), a biomarker of ovarian cancer.²⁰ The influence of incubation period on the detection limit is studied in the evaluation of the possibility of incubation period-free detection.

EXPERIMENTAL SECTION

Chemicals and Solutions. Biotinylated anti-CA-125 IgG (61R-C112BBT), anti-CA-125 IgG (10R-C112C), target CA-125 (30C-CP9062), and human serum (90R-106X) were obtained from Fitzgerald, Inc. (Acton, MA, USA). Antibody-GOx conjugation kit (ab102887) was purchased from Abcam, Inc. (Cambridge, MA, USA). GOx-conjugated anti-CA-125 IgG was prepared in phosphate buffer (50 mM, pH 7.4) according to the manufacturer's procedure. Avidin, $\text{Ru}(\text{NH}_3)_6^{3+}$, glucose, bovine-serum albumin (BSA), and all reagents for buffer solutions were obtained from Sigma-Aldrich, Co. Tris buffer comprised 50 mM tris(hydroxymethyl)aminomethane. Phosphate-buffered saline (PBS, pH 7.4) comprised 10 mM phosphate, 0.138 M NaCl, and 2.7 mM KCl. PBSB comprised all of the constituents of PBS in addition to 1% (w/v) BSA. The rinsing buffer (pH 7.6) contained 50 mM tris(hydroxymethyl)-

aminomethane, 40 mM HCl, 0.05% (w/v) BSA, and 0.5 M NaCl.

Preparation of Immunosensing Surface and Procedure for CA-125 Detection. Indium–tin oxide (ITO) electrodes were obtained from Samsung Corning (Daegu, Korea). ITO electrodes (1 cm × 2 cm each) were cleaned and pretreated using 0.1 M HCl solution.¹⁰ Avidin- and BSA-modified ITO electrodes were prepared as reported previously.^{21,22} Binding of the target CA-125 to the immunosensing electrodes was performed by treating the immunosensing electrodes with different concentrations of the target. Subsequently, the electrodes were treated with GOx-conjugated anti-CA-125 IgG. Biotinylated anti-CA-125 IgG was immobilized on the electrode by dropping 80 μL of a PBSB solution containing 10 $\mu\text{g}/\text{mL}$ biotinylated anti-CA-125 IgG onto the avidin- and BSA-modified ITO electrodes. The electrodes were maintained in the treated state for 30 min at 4 °C and then washed twice with rinsing buffer. The resulting electrodes were stored at 4 °C before use. Binding of target CA-125 IgG to the immunosensing electrodes was achieved by dropping 80 μL of human-serum solutions containing different concentrations of CA-125 onto the immunosensing electrodes. The electrodes were maintained in the treated state for 30 min at 4 °C and then washed twice with rinsing buffer. Subsequently, an 80 μL aliquot of a PBS solution containing 10 $\mu\text{g}/\text{mL}$ GOx-conjugated anti-CA-125 IgG was dropped onto the target-treated electrodes, and the electrodes were maintained in this state for 30 min at 4 °C and then washed twice with PBS.

Teflon electrochemical cells were assembled using an ITO electrode, an Ag/AgCl (3 M NaCl) reference electrode, and a platinum counter electrode. Two separate Tris-buffer solutions containing glucose and $\text{Ru}(\text{NH}_3)_6^{3+}$ were injected into a vessel of the cell and thoroughly mixed. The exposed geometric area of the ITO electrode was ca. 0.28 cm^2 . Incubation for enzymatic reactions was performed at 25 °C, and electrochemical measurements were carried out using a CHI 405A or CHI 708C (CH Instruments, Austin, TX, USA) apparatus.

RESULTS AND DISCUSSION

Figure 1a shows a schematic diagram of CA-125 detection using enzyme label-based EN redox cycling. GOx, $\text{Ru}(\text{NH}_3)_6^{3+}$, and glucose, respectively, act as an enzyme label, a redox mediator, and a substrate. In the presence of the GOx-conjugated IgG attached to the immunosensing electrode, $\text{Ru}(\text{NH}_3)_6^{3+}$ is reduced to $\text{Ru}(\text{NH}_3)_6^{2+}$ and glucose is oxidized to gluconic acid. $\text{Ru}(\text{NH}_3)_6^{2+}$ is oxidized back to $\text{Ru}(\text{NH}_3)_6^{3+}$ at the electrode. Repetition of this EN redox cycling for some extended period can give rise to high chronocoulometric charges. To obtain higher signal levels, the electrooxidation of $\text{Ru}(\text{NH}_3)_6^{2+}$, the enzymatic reduction of $\text{Ru}(\text{NH}_3)_6^{3+}$, and the enzymatic oxidation of glucose should be very fast (Figure 1a). In particular, the enzymatic reduction of $\text{Ru}(\text{NH}_3)_6^{3+}$ should be sufficiently rapid in air-saturated solution to compete with the enzymatic reduction of O_2 (Figure 1b), which is a rapid and competitive process.²³ ITO was selected for use as electrodes given that ITO electrodes facilitate low and reproducible capacitive background current/charge^{10,21} and the redox couple of $\text{Ru}(\text{NH}_3)_6^{3+}/\text{Ru}(\text{NH}_3)_6^{2+}$ undergoes a fast outer-sphere electron-transfer reaction even at the low electrocatalytic ITO electrodes.¹⁰ On the other hand, to obtain low background levels in the absence of the GOx-conjugated IgG, the direct electrooxidation of glucose at the electrode and the direct electron-transfer reaction between glucose and $\text{Ru}(\text{NH}_3)_6^{3+}$ (Figure 1c) should be slow. These basic requirements were investigated prior to the application of the GOx-based EN redox cycling system to CA-125 detection.

Cyclic voltammograms obtained using the ITO electrodes in Tris buffer (pH 8.0) are presented in Figure S1 in the Supporting Information. The voltammograms of the solution containing glucose and $\text{Ru}(\text{NH}_3)_6^{2+}$ (curve ii of Figure S1 in the Supporting Information) and of the solution containing only $\text{Ru}(\text{NH}_3)_6^{2+}$ (curve i of Figure S1 in the Supporting Information) were essentially similar, whereas the voltammogram for the solution containing glucose, GOx, and $\text{Ru}(\text{NH}_3)_6^{2+}$ (curve iii of Figure S1 in the Supporting Information) exhibited higher anodic currents than that for the solution of glucose and $\text{Ru}(\text{NH}_3)_6^{2+}$ (curve ii of Figure S1 in the Supporting Information). These results reveal that the direct electron-transfer reaction between glucose and $\text{Ru}(\text{NH}_3)_6^{3+}$ was not significant and that GOx-based EN redox cycling was active.

For further evaluation of these findings, chronocoulograms were obtained at 0.05 V at the ITO electrodes (Figure 2 and Figure S2 in the Supporting Information). Because the applied potential of 0.05 V is much higher than the formal potential of $\text{Ru}(\text{NH}_3)_6^{3+}/\text{Ru}(\text{NH}_3)_6^{2+}$ (ca. -0.15 V) that undergoes a fast outer-sphere electron-transfer reaction, the chronocoulometric charge (or chronoamperometric current) related to $\text{Ru}(\text{NH}_3)_6^{2+}$ electrooxidation is controlled only by mass transfer of $\text{Ru}(\text{NH}_3)_6^{2+}$ to the electrode not by the kinetics of $\text{Ru}(\text{NH}_3)_6^{2+}$ electrooxidation. Figure 2 and Figure S2 in the Supporting Information show that the anodic charges for a solution of glucose (curve i of Figure 2), a solution of $\text{Ru}(\text{NH}_3)_6^{3+}$ (curve ii of Figure S2 in the Supporting Information), and a solution of GOx (curve iii of Figure S2 in the Supporting Information) were slightly higher than the anodic charges for Tris buffer (curve i of Figure S2 in the Supporting Information). Moreover, the anodic charges for mixed solutions of two species (curves ii and iii of Figure 2 and curve iv of Figure S2 in the Supporting Information) were also

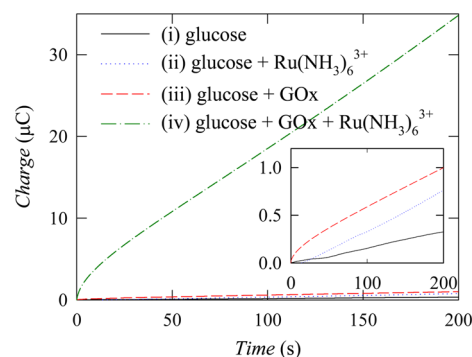


Figure 2. Chronocoulograms obtained at 0.05 V using ITO electrodes in air-saturated Tris buffer (pH 8.0) containing (i) 2.0 mM glucose, (ii) 2.0 mM glucose and 1.0 mM $\text{Ru}(\text{NH}_3)_6^{3+}$, (iii) 2.0 mM glucose and 100 $\mu\text{g/mL}$ GOx, or (iv) 2.0 mM glucose, 100 $\mu\text{g/mL}$ GOx, and 1.0 mM $\text{Ru}(\text{NH}_3)_6^{3+}$. A magnified view of the three chronocoulograms (curves i, ii, and iii) is presented in the inset.

slightly higher than those for Tris buffer (curve i of Figure S2 in the Supporting Information). These results indicate that the direct electrooxidation of glucose is slow at the ITO electrodes and that the direct electron-transfer reaction between glucose and $\text{Ru}(\text{NH}_3)_6^{3+}$ is also slow. Importantly, the charges for the solution of glucose, GOx, and $\text{Ru}(\text{NH}_3)_6^{3+}$ (curve iv of Figure 2) were much higher than those for the solution of glucose and $\text{Ru}(\text{NH}_3)_6^{3+}$ (curve ii of Figure 2). These results clearly demonstrate that the anodic charges due to the GOx-based EN redox cycling are significant. Interestingly, the evidence for EN redox cycling was more prominent in the chronocoulograms than in the cyclic voltammograms. This is due to the fact that although the difference between two electrochemical signals in cyclic voltammetry (or chronoamperometry) is small at any given moment, the difference is integrated in chronocoulometry, resulting in a large difference over time.

It is known that the reaction between reduced GOx and dissolved O_2 is much faster than that between reduced GOx and $\text{Ru}(\text{NH}_3)_6^{3+}$.²³ Nevertheless, the chronocoulograms illustrated that the EN redox cycling using $\text{Ru}(\text{NH}_3)_6^{3+}$ was considerable in air-saturated Tris buffer. The kinetics of the reaction between reduced GOx and $\text{Ru}(\text{NH}_3)_6^{3+}$ was evaluated on the basis of the rate constant, k (shown in Figure 1a). By making the initial concentration of $\text{Ru}(\text{NH}_3)_6^{3+}$ ($C_{\text{Ru}(\text{NH}_3)_6^{3+}}$) much smaller than that of glucose to ensure that GOx exists completely in reduced form in the steady state, k can be calculated from the limiting current (I_{lim}) in the chronoamperogram. I_{lim} is represented by^{4,11}

$$I_{\text{lim}} = F A C_{\text{Ru}(\text{NH}_3)_6^{3+}} \sqrt{2 D_{\text{Ru}(\text{NH}_3)_6^{2+}} k C_{\text{GOx}}} \quad (1)$$

where F is the Faraday constant, A is the electrode area (0.28 cm^2), $D_{\text{Ru}(\text{NH}_3)_6^{2+}}$ is the diffusion coefficient of $\text{Ru}(\text{NH}_3)_6^{2+}$ (ca. $1 \times 10^{-5} \text{ cm}^2/\text{s}$),²⁴ and C_{GOx} is the concentration of GOx. An average background-corrected I_{lim} of 70 nA at 100 s (Figure S3 in the Supporting Information) was achieved when the chronocoulogram was acquired in air-saturated Tris buffer (pH 8.0) containing 0.1 mM $\text{Ru}(\text{NH}_3)_6^{3+}$, 100 $\mu\text{g/mL}$ (6.25 μM) GOx, and 20 mM glucose. The k value calculated from eq 1 was ca. $5 \times 10^1 \text{ M}^{-1}\text{s}^{-1}$, which is comparable to or slightly lower than the reported values that were obtained in deoxygenated solutions,^{11,23} which clearly demonstrates that k is considerable even in the presence of dissolved O_2 .

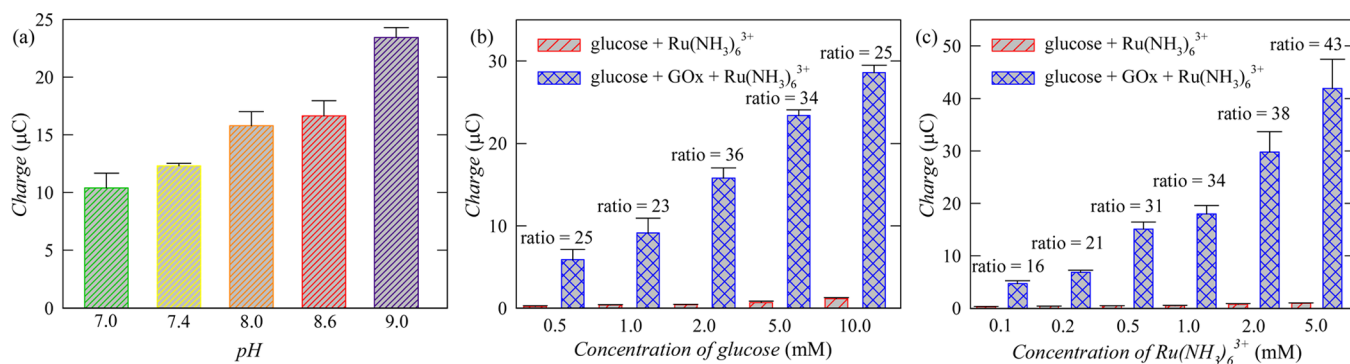


Figure 3. (a) Histogram of the pH dependence of the charges at 100 s in chronocoulograms that were obtained at 0.05 V using ITO electrodes in air-saturated Tris buffer containing 2.0 mM glucose, 100 μg/mL GOx, and 1.0 mM Ru(NH₃)₆³⁺. (b) Histogram of the glucose-concentration dependence of the charges at 100 s in chronocoulograms that were obtained at 0.05 V using ITO electrodes in air-saturated Tris buffer (pH 8.0) containing either glucose and 1.0 mM Ru(NH₃)₆³⁺ or glucose, 100 μg/mL GOx, and 1.0 mM Ru(NH₃)₆³⁺. (c) Histogram of the Ru(NH₃)₆³⁺-concentration dependence of the charges at 100 s in chronocoulograms that were obtained at 0.05 V using ITO electrodes in air-saturated Tris buffer (pH 8.0) containing either 2.0 mM glucose and Ru(NH₃)₆³⁺ or 2.0 mM glucose, 100 μg/mL GOx, and Ru(NH₃)₆³⁺. The ratio corresponds to the ratio of the charge in the presence of GOx to the charge in the absence of GOx.

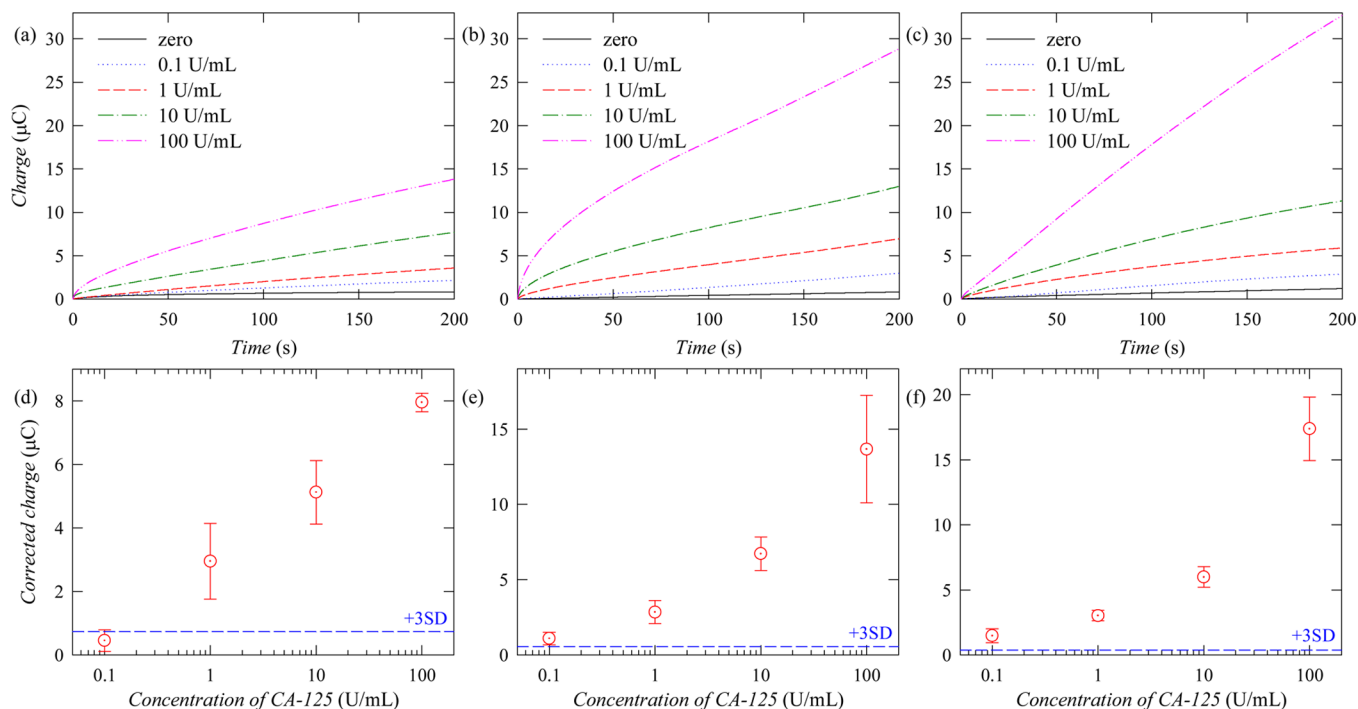


Figure 4. (a, b, c) Chronocoulograms obtained at 0.05 V for various concentrations of CA-125 after incubation of the final immunosensing electrodes in air-saturated Tris buffer (pH 8.0) containing 2.0 mM glucose, 100 μg/mL GOx, and 1.0 mM Ru(NH₃)₆³⁺ for (a) 0, (b) 5, or (c) 10 min. (d, e, f) Calibration plots: concentration dependence of the charges at 100 s in panels a, b, and c. Each concentration experiment was carried out with 3 different sensing electrodes for assay of the same sample. All of the data were corrected by the mean value of seven measurements determined at a concentration of zero. The dashed line corresponds to three times the standard deviation (SD) of the charge at a concentration of zero. The error bars represent the SD of the three measurements.

The pH dependence of the GOx-based EN redox cycling is shown in Figure 3a. The charge observed at 100 s in the chronocoulogram increased with increasing pH. The formal potential of Ru(NH₃)₆³⁺/Ru(NH₃)₆²⁺ is independent of pH given that H⁺ and OH[−] ions are not involved in the redox reaction, whereas the formal potential of the redox center of GOx decreases with increasing pH. Moreover, the formal potential of Ru(NH₃)₆³⁺/Ru(NH₃)₆²⁺ is higher than that of the redox center of GOx. Therefore, the difference between the two formal potentials of Ru(NH₃)₆³⁺/Ru(NH₃)₆²⁺ and the redox center of GOx increases with increasing pH. This increased

potential difference appears to facilitate faster EN redox cycling. Given that Ru(NH₃)₆³⁺ is more stable near neutral pH, a pH of 8 was selected for the immunosensing experiments. The dependence of the signal level and background level in the GOx-based EN redox cycling on the glucose concentration is shown in Figure 3b. The charge measured in both the presence and absence of GOx increased with increasing glucose concentration. The highest signal-to-background ratio was achieved at a glucose concentration of 2.0 mM, which was thus selected as the optimum glucose concentration. Figure 3c shows the dependence of the signal level and background level

in the GOx-based EN redox cycling on the $\text{Ru}(\text{NH}_3)_6^{3+}$ concentration. The signal-to-background ratio increased with increasing $\text{Ru}(\text{NH}_3)_6^{3+}$ concentration. However, the standard deviation of the signal was quite high at high $\text{Ru}(\text{NH}_3)_6^{3+}$ concentrations. Therefore, a $\text{Ru}(\text{NH}_3)_6^{3+}$ concentration of 1.0 mM was selected for the immunosensing experiments.

In a prior report, we demonstrated that the nonspecific binding of proteins on avidin- and BSA-modified ITO electrodes is negligible.²¹ The nonspecific binding of GOx-conjugated IgG on similar electrodes was also investigated, demonstrating that the nonspecific binding was not significant when a solution of GOx-conjugated IgG was dropped on an avidin- and BSA-modified ITO electrode (Figure S4 in the Supporting Information).

The EN redox cycling using glucose, GOx, and $\text{Ru}(\text{NH}_3)_6^{3+}$ was applied to the detection of CA-125. Figure 4a–c shows the chronocoulograms acquired for various concentrations of CA-125. Two solutions (a solution of glucose and a solution of $\text{Ru}(\text{NH}_3)_6^{3+}$) were mixed in the vessel of an electrochemical cell, and respective samples were subjected to three incubation periods (0, 5, and 10 min corresponding to Figure 4a–c, respectively) prior to the electrochemical measurements. Very importantly, the charges obtained for an incubation period of 0 min (Figure 4a) were comparable to those obtained for incubation periods of 5 and 10 min (Figure 4b,c). The detection limits were calculated from the calibration plots in Figure 4d–f, which were obtained from the chronocoulograms in Figure 4a–c at 100 s. The detection limit for the incubation period of 0 min was slightly higher than 0.1 U/mL: 0.15 U/mL after a regression curve was fitted; the detection limits for the incubation periods of 5 and 10 min were slightly lower than 0.1 U/mL: 0.05 and 0.02 U/mL, respectively, after regression curves were fitted. Although the detection limit for the incubation period of 0 min was higher than those for the longer incubation periods, the detection limits were largely similar. The detection limit of 0.1 U/mL is similar to or less than the previously reported values in the electrochemical detection based on a change in interfacial electron transfer (0.1 U/mL),²⁵ the competitive electrochemical detection using direct electrochemistry of HRP (1.29 U/mL),²⁶ the electrochemical detection using electric field-driven incubation (0.1 U/mL),²⁷ and the micelle-based sandwich-type fluorescence detection (0.15 U/mL),²⁸ indicating that the proposed immunosensor is highly sensitive.

CONCLUSIONS

This study demonstrates that the incubation period for catalytic reactions of enzyme labels can be effectively minimized in the electrochemical immunosensor employing GOx label-based EN redox cycling. The need for an incubation period was effectively negated and high signal-to-background ratios were achieved because of the rapid electron transfer between the electrode and the GOx label mediated by $\text{Ru}(\text{NH}_3)_6^{3+}$, along with the acquisition of chronocoulometric charges at a potential in the mass transfer-controlled region. The detection limit for CA-125 for the incubation period of 0 min was slightly higher than 0.1 U/mL. The immunosensing scheme is of practical importance given that the total immunosensing time can be reduced without a large increase in the detection limit.

ASSOCIATED CONTENT

Supporting Information

More supporting data. This material is available free of charge via the Internet at <http://pubs.acs.org>.

AUTHOR INFORMATION

Corresponding Author

*E-mail: hyang@pusan.ac.kr.

Notes

The authors declare no competing financial interest.

ACKNOWLEDGMENTS

This research was supported by the National Research Foundation of Korea (2010-0020772, 2012R1A2A2A06045327, 2012-M3C1A1-048860, and 2005-01333).

REFERENCES

- (1) Scheller, F. W.; Bauer, C. G.; Makower, A.; Wollenberger, U.; Warsinke, A.; Bier, F. F. Immunoassays Using Enzymatic Amplification Electrodes. In *Biomolecular Sensors*; Gizeli, E., Lowe, C. R., Eds.; Taylor & Francis Ltd.: New York, 2002; pp 207–238.
- (2) Warsinke, A. *Adv. Biochem. Eng./Biotechnol.* **2008**, *109*, 155–193.
- (3) Yang, H. *Curr. Opin. Chem. Biol.* **2012**, *16*, 422–428.
- (4) Bourdillon, C.; Demaille, C.; Moiroux, J.; Savéant, J.-M. *Acc. Chem. Res.* **1996**, *29*, 529–535.
- (5) Chen, D.; Wang, G.; Li, J. *J. Phys. Chem. C* **2007**, *111*, 2351–2367.
- (6) Liu, G.; Wan, Y.; Gau, V.; Zhang, J.; Wang, L.; Song, S.; Fan, C. *J. Am. Chem. Soc.* **2008**, *130*, 6820–6825.
- (7) Limoges, B.; Marchal, D.; Mavre, F.; Savéant, J. *J. Am. Chem. Soc.* **2006**, *128*, 2084–2092.
- (8) Haque, A.-M. J.; Park, H.; Sung, D.; Jon, S.; Choi, S.-Y.; Kim, K. *Anal. Chem.* **2012**, *84*, 1871–1878.
- (9) Chen, P.; McCreery, R. L. *Anal. Chem.* **1996**, *68*, 3958–3965.
- (10) Choi, M.; Jo, K.; Yang, H. *Bull. Korean Chem. Soc.* **2013**, *34*, 421–425.
- (11) Chen, L.; Gorski, W. *Anal. Chem.* **2001**, *73*, 2862–2868.
- (12) Nakabayashi, Y.; Hirotsaki, Y.; Yamauchi, O. *Inorg. Chem. Commun.* **2006**, *9*, 935–938.
- (13) Ryabova, E. S.; Goral, V. N.; Csöregi, E.; Mattiasson, B.; Ryabov, A. D. *Angew. Chem., Int. Ed.* **1999**, *38*, 804–807.
- (14) Sekretaryova, A. N.; Vokhmyanina, D. V.; Chulanova, T. O.; Karyakina, E. E.; Karyakin, A. A. *Anal. Chem.* **2012**, *84*, 1220–1223.
- (15) Lai, G.; Yan, F.; Ju, H. *Anal. Chem.* **2009**, *81*, 9730–9736.
- (16) Zhang, J.; Pearce, M. C.; Ting, B. P.; Ying, J. Y. *Biosens. Bioelectron.* **2011**, *27*, 53–57.
- (17) Hosoda, H.; Tsukamoto, R.; Shoriken, K.; Takasaki, W.; Nambara, T. *Chem. Pharm. Bull.* **1988**, *36*, 1808–1813.
- (18) Le Goff, G. C.; Blum, L. J.; Marquette, C. A. *Anal. Chem.* **2011**, *83*, 3610–3615.
- (19) Zeravik, J.; Ruzgas, T.; Fránek, M. *Biosens. Bioelectron.* **2003**, *18*, 1321–1327.
- (20) Gunawardana, C. G.; Kuk, C.; Smith, C. R.; Batruch, I.; Soosaipillai, A.; Diamandis, E. P. *J. Proteome Res.* **2009**, *8*, 4705–4713.
- (21) Akanda, M. R.; Aziz, M. A.; Jo, K.; Tamilavan, V.; Hyun, M. H.; Kim, S.; Yang, H. *Anal. Chem.* **2011**, *83*, 3926–3933.
- (22) Akanda, M. R.; Choe, Y. L.; Yang, H. *Anal. Chem.* **2012**, *84*, 1049–1055.
- (23) Morris, N. A.; Cardosi, M. F.; Bircb, B. J.; Turner, A. P. F. *Electroanalysis* **1992**, *4*, 1–9.
- (24) Wang, Y.; Limon-Petersen, J. G.; Compton, R. G. *J. Electroanal. Chem.* **2011**, *652*, 13–17.
- (25) Das, J.; Kelley, S. O. *Anal. Chem.* **2011**, *83*, 1167–1172.
- (26) Dai, Z.; Yan, F.; Chen, J.; Ju, H. *Anal. Chem.* **2003**, *75*, 5429–5434.

- (27) Mouffouk, F.; Chishti, Y.; Jin, Q.; Rosa, M. E.; Rivera, M.; Dasa, S.; Chen, L. *Anal. Biochem.* **2008**, *372*, 140–147.
- (28) Wu, J.; Yan, Y.; Yan, F.; Xu, H. *Anal. Chem.* **2008**, *80*, 6072–6077.